How to Cite: Mamytbekov, G.K., Beksultanov, Zh.I., Bannykh, V.I., & Dan'ko, I.V. (2022) Synthesis, Structure and Properties of Hybrid Composite Bentonite-Based Materials. *Bulletin of the University of Karaganda – Chemistry.* https://doi.org/10.31489/2022Ch3/3-22-21

Article Received: 7 June 2022 | Revised: 11 July 2022 | Accepted: 15 July 2022 | Published online: 26 July 2022

UDC 541.64:539.2:532.135 https://doi.org/10.31489/2022Ch3/3-22-21

G.K. Mamytbekov, Zh.I. Beksultanov, V.I. Bannykh, I.V. Dan'ko

Institute of Nuclear Physics, Almaty, Kazakhstan
*(*Corresponding author's e-mail: g.mamytbekov@inp.kz)*

Synthesis, Structure and Properties of Hybrid Composite Bentonite-Based Materials

A systematic study of the synthesis of hybrid composite materials based on synthetic (poly-N-vinylpyrrolidone) and natural (agar-agar) macromolecules in the presence of plasticizers (PEG-400, glycerin) and mineral filler bentonite has been performed by the method of electron irradiation. The methods of X-ray diffraction analysis and SEM showed that the structure of the resulted hybrid compositions is defined as an interpenetrating network with the distributed intercalated particles of mineral component inside its volume. It has been established that mechanical properties of the hybrid composition are determined mainly by the structural organization of the interpenetrating polymer network, formed during electron irradiation of the initial polymer mixture in the presence of plasticizers, as well as by the conditions for intercalation of polymer segments into the interpacket layers of the mineral matrix. During the process of crazing of the sample under tension the shear stress is concentrated in the central part of the sample from the periphery of the fastening. It is shown that the degree of swelling for hybrid composition strongly depends on concentration of a low molecular plasticizer in the polymeric interpenetrating network, which can easily impregnate into the interplanar layers of bentonite.

Key words: hybrid composition material (HCM), polymer-inorganic compositions (PIC), electron irradiation, synthetic and natural polymers, bentonite, deformation, compression, tension, intercalation, interpenetrating networks (IPN).

Introduction

Hybrid nanocomposites represent a promising class of complex polymer-inorganic materials in which mineral particles are distributed in a polymer matrix of synthetic or natural origin [1–3]. The interphase boundary between the filler and the polymer matrix in nanocomposites occupies a larger area than in conventional microcomposites; therefore, it affects the properties of nanocomposites to a much greater extent even with a minimum amount of filler [4].

Among the variety of hybrid nanocomposites, a special place is occupied by systems where bentonite clays are used as an inorganic filler. The study of structure and properties of minerals of the layered aluminosilicates class, produced from available and widespread natural raw materials, is an important scientific and practical task aimed to create new multifunctional materials [5, 6]. This is mainly defined by uniqueness of the physical-chemical properties of layered aluminosilicates, which appear in a developed specific surface, the presence of active reaction centers, high adsorption and ion exchange abilities [7–9]. This suggests the possibility of using bentonite clays in medicine as drug carriers in the form of gel, film and injectable drug forms [10]. The main conditions for the use of polymer-clay composite materials for medical purposes are: uniformity of the clay mineral composition, harmlessness of the components and relative indifference of their behavior in the polymer matrix.

There are a lot of publications devoted to the synthesis of polymer-clay systems based on natural and synthetic polymers [11–13], where the possibilities of designing new classes of hybrid polymer-inorganic compositions for solving various applied and technological problems are considered in detail.

Depending on the nature of used components (for example, chain, layered or zeolite silicate, polymer matrix) and the method of preparation, three main types of hybrid compositions can be produced in which layered silicates are bonded to the polymer matrix in various ways [13–15]: the first case when the polymer cannot intercalate between silicate layers resulting in formation of a microcomposite with separated phases. The second type of polymer compositions occurs when intercalation or exfoliation of the clay takes place, in which a single extended polymer chain is inserted between the silicate layers, which leads to formation of alternating layers of polymer and silicate particles. In the third case, the silicate layer is evenly and completely dispersed in a continuous polymer medium, resulting in a completely layered exfoliated structure.

The purpose of this paper is to review the mechanism of formation and structure of intercalated hybrid composite materials based on natural (agar-agar, bentonite) and synthetic medical-purpose polymers (poly-N-vinylpyrrolidone, PVP) in the presence of low and high molecular plasticizers (glycerol, polyethylene glycol PEG-400) produced by the method of electron irradiation.

The method of electron irradiation was used to obtain three-dimensional polymer structures due to the radiation cross-linking of polyvinylpyrrolidone macromolecules. Other options for cross-linking of a linear PVP are possible only by means of thermal degradation at the temperature of decomposition of the material at a temperature above 120 °C in a dry state, which is not acceptable for our purposes. Moreover, the electron irradiation is a pure reagent-free method for obtaining three-dimensional polymer systems, that solves the issue of sterilization of polymer compositions, which is the main condition for their application in medical practice for use as an anti-burn and an anti-bedsore hydrogel coated on damaged tissue.

Experimental

Bentonite (BT) from the JSC “Ilsky plant Utyazhelitel” (Russia) TU-2164-003-00136716-2015 was used after washing with distilled water and drying to constant weight at a temperature of 70 °C.

Agar-agar (AA) “Grasar” 900 (Company “Bargus Trade”, Russia) is a white fine powder, manufactured in accordance with STO 010-96140533-2016, was used with no additional purification.

Poly-N-vinylpyrrolidone (PVP) (Kollidon 90 F) and PEG400 (BASFPharma, Germany) were used with no additional purification.

Preparation of a composite hydrogel solution included two stages: 1) dissolution of the required weight of PVP at a temperature of 15 °C with stirring on a magnetic stirrer until complete dissolution, after which plasticizer PEG-400 (P1) was added to this solution. Separately, a solution of agar-agar (P2) was prepared in distilled water at a temperature of 80–90 °C for 2 hours. Next, solutions P1 and P2 were mixed with addition of 0.5 g (0.5 %) of dry bentonite powder with vigorous stirring until a homogeneous system with a uniform distribution of the mineral component (for 1–2 hours) was obtained until a suitable temperature (40–45 °C) is reached for pouring the polymer-mineral mixture into the special shaped containers.

Irradiation of a mixture of prepared solutions of polymer-inorganic compositions (PIC) of a given composition was performed in an accelerator ILU-10 with electron beam in the dose range from 5 to 25 kGy in special plastic molds with a rectangular cross section of 10×12 cm·or in cylindrical ampoules with an inner diameter of 10 mm and a height 30 mm with the following processing mode: E — 5 MeV, I_{imp} — 350 mA; f — 26 Hz, V — 2.7 cm/s; I_{av} — 4.55 mA. The samples, obtained at the irradiation dose of 25 kGy, were used in the work.

X-ray diffraction analysis (XRD) was performed on a Bruker X-ray diffractometer with CuK_α radiation. A thin dried film of a hybrid composition and powdered bentonite up to 10 μm in size were scanned in the 2θ angle range from 20° to 70° with a step of 0.02°, a scanning speed of 2 s/point, with radiation parameters of 40 kV and 40 mA.

Scanning electron microscopy (SEM) was performed using a Hitachi model TM 4000 Plus microscope (Japan) equipped with an X-ray fluorescence energy dispersive analysis (EDS) attachment with a crystal detector. Samples were studied under low vacuum in back-scattered electron (BSE) mode.

IR-Fourier spectra were taken on a spectrometer Carry 660 (Agilent, USA) in the absorption mode in the frequency range 700–4000 cm^{-1} with a resolution of 4 cm^{-1}.

The mechanical properties of PIC samples were analyzed on a texture analyzer TAXTplusStableMicroSystems (England) with software. The principle of the texture analyzer is that the sample is subjected to the action of controlled forces using a probe while stretching a rectangular sample or compressing a cylindrical sample. The resistance of a material to tensile or compressive forces is measured using a torque sensor.

Results and Discussion

In our previous study [16], we considered the mechanism for formation of rare cross-linked composite hydrogels based on the natural polysaccharide agar-agar, a synthetic polymer for medical application, poly-N-vinylpyrrolidone (PVP), synthesized by electron irradiation. It has been established that synthesis conditions and component composition of the initial mixture determine the structure and morphology of the formed hydrogel compositions and their mechanical properties. A new interpretation of the formation of the composite hydrogels structure in the presence of various plasticizers was provided. It was shown that formation of a three-dimensional structure of PVP occurs as a result of electron irradiation of the reaction mixture in an aqueous medium in the presence of low- and high-molecular plasticizers, the content of which can be controlled to obtain networks of various strengths and elasticity. The composite hydrogels P[AA-PVP-plasticizer] are a model of interpenetrating networks consisting of physical and covalent crosslinking points that provides them a good combination of an elastic and viscoelastic properties.

Considering above, this article reviews the mechanism for formation of intercolated structures of a natural mineral in the volume of a polymer matrix, synthesized by the method of electron irradiation of solutions of natural (AA) and synthetic (PVP) polymers mixtures in the presence of plasticizers. Content of the mineral filler was chosen equal to 0.5 wt.% in order to achieve a uniform distribution of natural silicate suspension in the volume of the polymer mixture solution while maintaining their aggregative stability.

It is known that the main rock-forming components of bentonite clays are minerals of the smectite group, mainly montmorillonites (more than 70 %). Their composition contains also quartz, feldspars, calcite and rarely pyrite, as well as other clay minerals such as illite, kaolinite, and mixed-layered minerals [8, 11, 15, 17, 18].

Figure 1 shows the X-ray diffraction patterns of bentonite powder (1) and its intercolated complex (ICC) in the form of a film, scanned in the range of slip angles 2θ from 18° to 90° with a step of 0.02°. The X-ray diffraction data of bentonite (curve 1) shows characteristic diffraction reflections at 20.96°, 26.75°, 29.51°, 31.8°, 42.46° and 61.54°, which correspond to the characteristic signals of quartz 20.96°, 26.75° with interplanar distances (d) of 4.23 Å and 3.32 Å, respectively, and oxides of calcium, magnesium and aluminum with frequent line overlap, which makes their identification difficult.

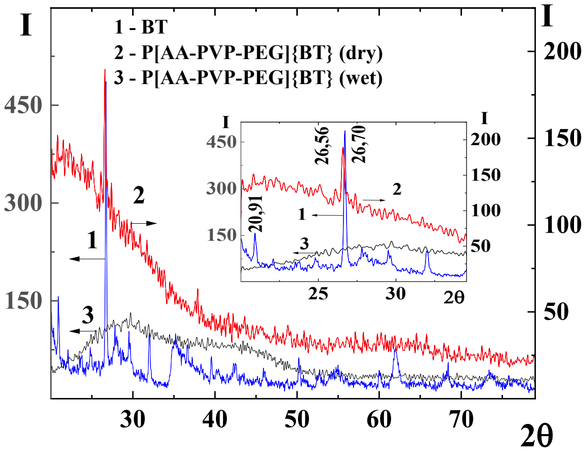

Figure 1. X-ray diffraction patterns of BT (1), (2) dry and (3) wet hybrid composition P[AA-PVP-PEG]{BT}

During intercalation of bentonite particles into the volume of the polymer matrix P[AA-PVP-PEG], the characteristic maximum of the diffraction signal of quartz in the composition of clay shifts from 26.75° to 26.58° with an increase in the interplanar distance from 3.380 Å to 3.342 Å, respectively. However, in this case, there is a significant expansion of the range of diffraction signals in the range of 2θ20-40 Å and the growth of their intensity observed for the hybrid composite material P[AA-PVP-PEG]{BT}, which may indicate in favor of splitting of the layered packing of the polyoxide forms of aluminum and silicon included in the composition of bentonite clay. In the case of wet compositions, expansion of the range of diffraction signals is observed in a wider range from 30° to 50°. Disappearance of a number of characteristic diffraction bands of pure bentonite in the case of its intercolation into the volume of polymer matrix is explained by a decrease in the content or disappearance of a number of basic and impurity compounds, for example, quartz (2θ = 50.14°, 59.94°) and montmorillonite itself (2θ = 68.12° and 68.31°), which may be caused by a complete filling of the interlayer space of the layered silicate with macromolecules of interpenetrating network. A detailed explanation of this assumption will be considered in the analysis of the SEM data.

It was previously noted [19, 20] that clay minerals are divided into two types depending on alternation of tetrahedral [SiO_2] and octahedral [AlO_6] sheets and their mutual arrangement in the crystal lattice: (i) 2:1 composition clay (smectite and montmorillonite) and (ii) 1:1 clay (kaolinite). The high size ratio of smectite clay minerals is defined by their unique intercalation-separation properties, making them especially important and effective as reinforcing fillers for polymers [4–6].

Bentonite clay is mainly composed of thin layers of 1 nm thick composition 2:1 aluminum phyllosilicates with a central octahedral alumina sheet fused between two outer tetrahedral silica sheets by shared oxygen atoms, forming galleries between the alternating layers (Figure 2) [18].

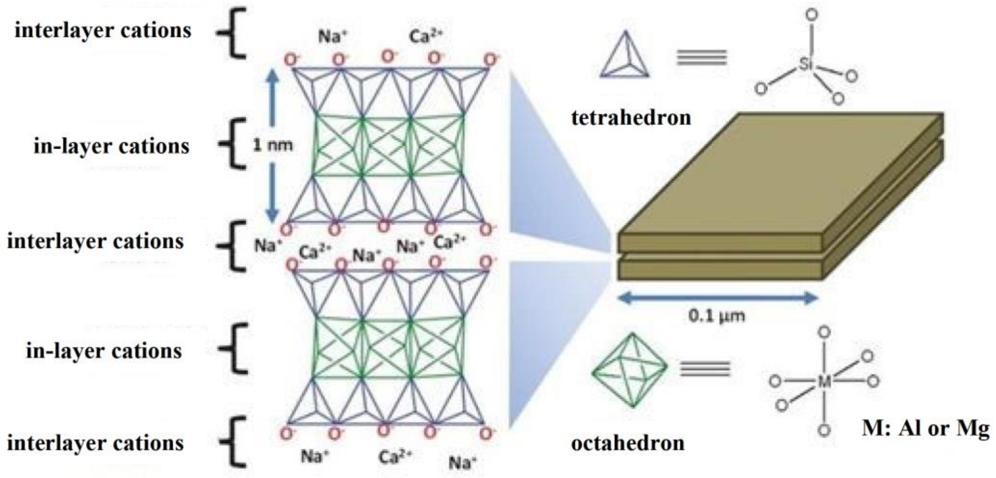

Figure 2. Structure of bentonite clay composition 2:1 [18]

The structured silicon and alumina layers are interconnected by covalent bonds, in which both the isomorphic substitution of silicon for aluminum in the tetrahedral chain and the substitution of aluminum in the octahedral layer for iron, magnesium or alkaline earth metals take place. In addition, in stabilization of the covalently bonded layers of bentonite, an essential role is played by the electrostatic forces of interaction that arise between the ions of alkali and alkaline earth metals or impurity transition metals located in the gallery between the tetrahedral layers, thus tightly holding the stacks of clay layers together from disintegration either in dry or in wet state. Under such conditions the covalent bonds between the interlayers of aluminosilicate sheets of the clay create difficulties to penetrate into their bulk for most hydrophobic macromolecules [17, 18] due to the high hydrophilicity of the mineral matrix.

Introduction of massive cations or anions into the interlayer space also contributes to loosening of the crystallite structure, which makes it possible for surfactants and water-soluble polymers to penetrate. This leads to complete splitting of crystallites into primary nanosized silicate plates, i.e. to exfoliation [18, 19, 21].

Figure 3a shows that bentonite particles represent a structure characterized by the presence of a complex non-oriented clay mass - a matrix, which contains randomly arranged dust-like sand grains that do not contact each other. When zoomed in from 120 (1) to 1000 (2) and 4000 (3) times, a clear picture of the surface structure of the layered and chain structure of natural polymer can be obtained.

This issue has been widely discussed in scientific publications and review articles [3, 4, 11, 17, 20, 21, 23]. The most researchers believe that the stage of modification of clay minerals with hydrophobizing or lyophilizing surfactants is necessary to obtain polymer-silicate (nano) compositions with acceptable mechanical characteristics and operational parameters, since surfactants are able to intercalate into the interlayer space of inorganic ionite with the formation of weak van der Waals (dispersion) or strong covalent chemical bonds.

The morphology of the polymer film is represented by macroporous segments with a developed surface and topological inhomogeneity typical of amorphous sparsely crosslinked polymer systems (Fig. 3b). It is characterized by a layered structure or cleavage of layers caused by formation of a matrix of an interpenetrating network with alternating layers of natural (agar-agar) and synthetic polymers (PVP) with lateral grafting of plasticizer molecules (PEG or glycerol), which we previously described in details in [15].

When forming a hybrid composition of bentonite-IPN, the picture changes significantly (Fig. 3c). It can be seen that the bentonite particles are unevenly distributed over the interlayer surfaces of the interpenetrating network. Particularly noteworthy is the shape of bentonite particles, which resemble the structure of γ-alumina. Traditionally, its crystal structure is described as feldspar, in which aluminum atoms are localized simultaneously in tetraeric and octahedral positions, as a result of which its surface is much more hydroxylated compared to silica gel. It has been noted that the presence of water accelerates the rate of aluminum hydrolysis with formation of a lamellar large-pore structure of aluminum hydroxide [22–26], which also has an octahedral structure.

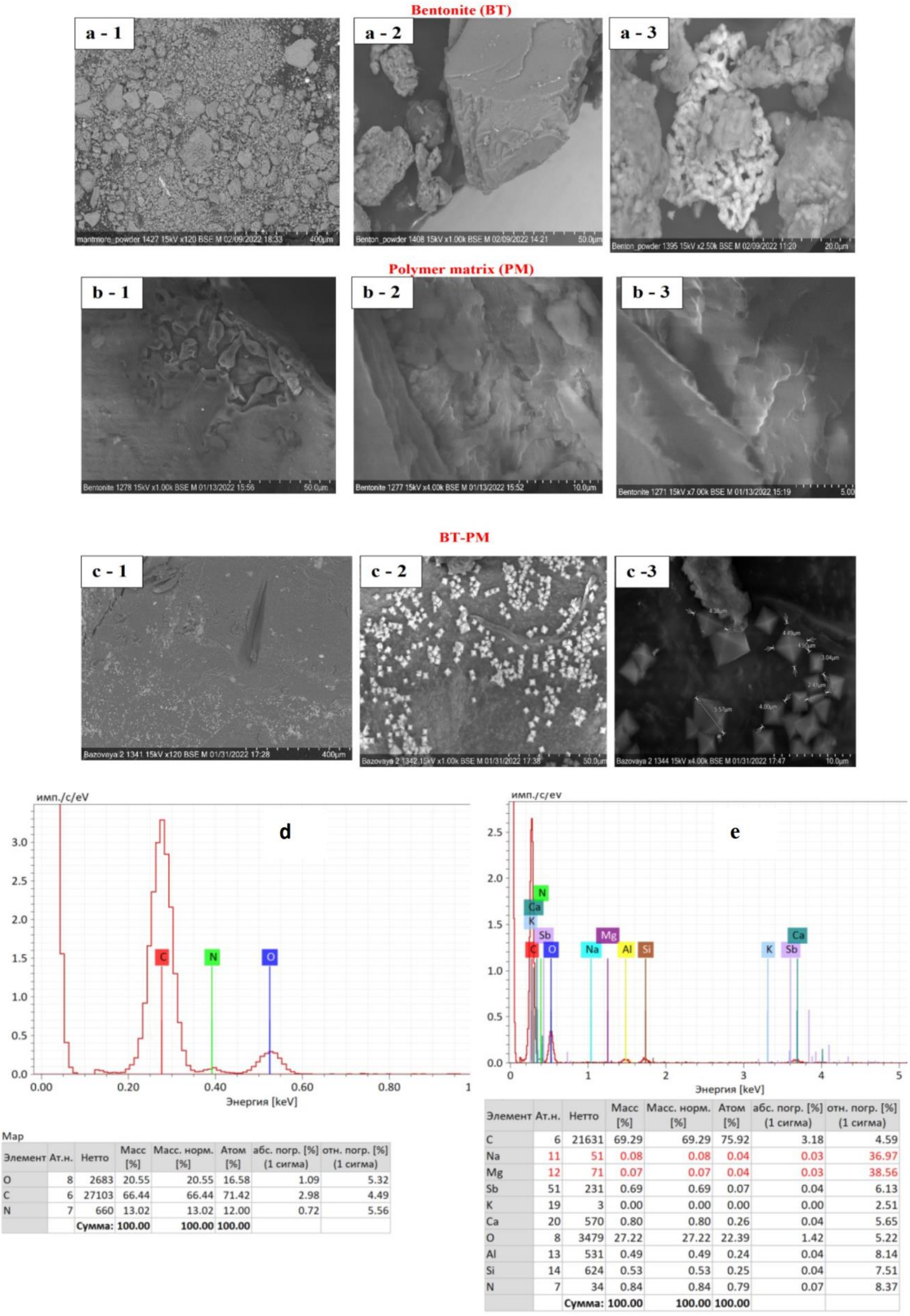

Map

Элемент	Ат.н.	Нетто	Масс [%]	Масс. норм. [%]	Атом [%]	абс. погр. [%] (1 сигма)	отн. погр. [%] (1 сигма)
O	8	2683	20.55	20.55	16.58	1.09	5.32
C	6	27103	66.44	66.44	71.42	2.98	4.49
N	7	660	13.02	13.02	12.00	0.72	5.56
		Сумма:	**100.00**	**100.00**	**100.00**		

Элемент	Ат.н.	Нетто	Масс [%]	Масс. норм. [%]	Атом [%]	абс. погр. [%] (1 сигма)	отн. погр. [%] (1 сигма)
C	6	21631	69.29	69.29	75.92	3.18	4.59
Na	11	51	0.08	0.08	0.04	0.03	36.97
Mg	12	71	0.07	0.07	0.04	0.03	38.56
Sb	51	231	0.69	0.69	0.07	0.04	6.13
K	19	3	0.00	0.00	0.00	0.00	2.51
Ca	20	570	0.80	0.80	0.26	0.04	5.65
O	8	3479	27.22	27.22	22.39	1.42	5.22
Al	13	531	0.49	0.49	0.24	0.04	8.14
Si	14	624	0.53	0.53	0.25	0.04	7.51
N	7	34	0.84	0.84	0.79	0.07	8.37
		Сумма:	**100.00**	**100.00**	**100.00**		

Figure 3. SEM micrographs of bentonite (a), P[AA-PVP-PEG] (b) and P[AA-PVP-PEG]{BT}(c) at various magnifications: *1* —120; *2* — 1000 and *3* — 4000 times and X-ray fluorescence energy dispersive analysis for P[AA-PVP-PEG] (d) and P[AA-PVP-PEG]{BT} (e).

This conclusion about the chemical structure of the hybrid compositions is in good agreement with the X-ray fluorescence energy dispersive analysis data for P[AA-PVP-PEG] (Fig. 3d) and P[AA-PVP-PEG]{BT} (Fig. 3e).

It should be assumed that we are dealing with the process of partial or complete delamination of sheets with a composition of 2:1 until the complete separation of the silica and alumina layers from each other due to the excess negative charge arising in the process of hydration. Sequential analysis of the stages of montmorillonite hydration confirms the fact that 1 to 4 layers of water molecules can be located in the spaces between silicate layers [27–29].

However, in the studied system the particle sizes determined according to SEM data go far beyond nanoscale, in particular, the average size along the diagonal of octahedrons varies from 3.04 to 5.57 μm, that is, it exceeds the interplanar distances between layers by three orders of magnitude (Fig. 1). Therefore, the alternative explanation can be provided, according to which, in addition to delamination or exfoliation of bentonite particles in the intertwined polymer matrix of the interpenetrating PVP-AA network, microcrystallites of bentonite particles grow into more or less large aggregates in the form of a single monolithic structure of the same geometry as for individual molecules of hydrated alumina in the form of well-formed octahedra.

In the presence of polymers with bulky side pyrrolidone rings (PVP) linked to plasticizer molecules (PEG or glycerol) through a system of hydrogen bonds, as well as polysaccharides which macromolecules consist of cyclic units of D-galactose and 3,6-anhydro-L-galactose, deep splitting of aluminosilicate sheets from each other should be expected (Fig. 4).

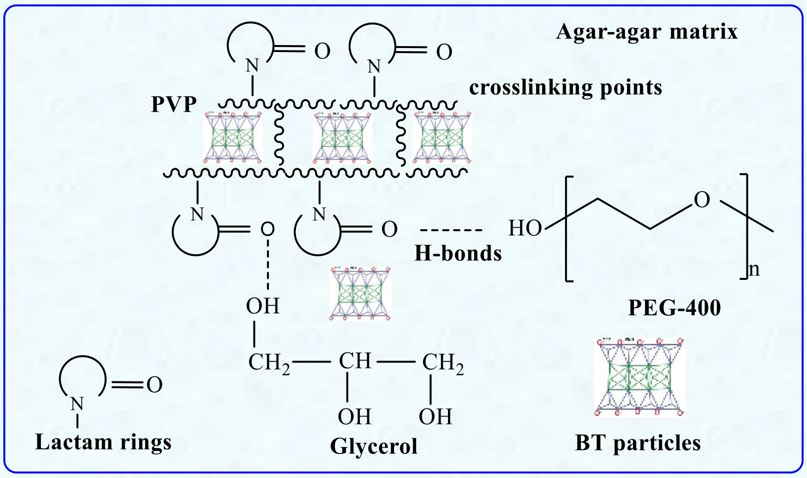

Figure 4. Schematic diagram of formation of composite hydrogels based on agar-agar and PVP in the presence of plasticizers by electron irradiation [15]

Thus, exfoliation begins with the splitting of sheets along the boundary of the gallery ≡Si-O-Al-O-Si≡ $|mMe^{n+}\cdot kH_2O|$ ≡Si-O-Al-O-Si≡ with subsequent destruction of the three-layer structure along the heterobond line ≡Si-O-Al along the oxygen atom. When bentonite particles are in a polymer matrix consisting of two complementary and intertwined macromolecules associated with the terminal hydroxyl groups of plasticizers, the exfoliation process can proceed until the complete rejection of not only sheets of aluminum phyllosilicates from each other, but also by splitting the structures of polyoxosilicon and polyoxoaluminum chains into separate fragments in the form of disparate γ-Al_2O_3 octahedron, as shown in Figure 5.

An increase in the interlayer space during exfoliation of silicates by the IPN matrix contributes to the further process of delamination of the layered filler due to growth of disjoining pressure between the packages and, subsequently, between the sheets of the packages (Fig. 5). The irradiation of the system with an electron beam exacerbates this process since the action of various types of radiation leads to the formation of radiation defects [30]. In this case occurs an uncontrolled redistribution of crosslinking sites and dimensions of the pore structures of the polymer matrix, where more or less hydrated bentonite particles are initially located according to the law of average distribution with nonlinear effects during structural transitions.

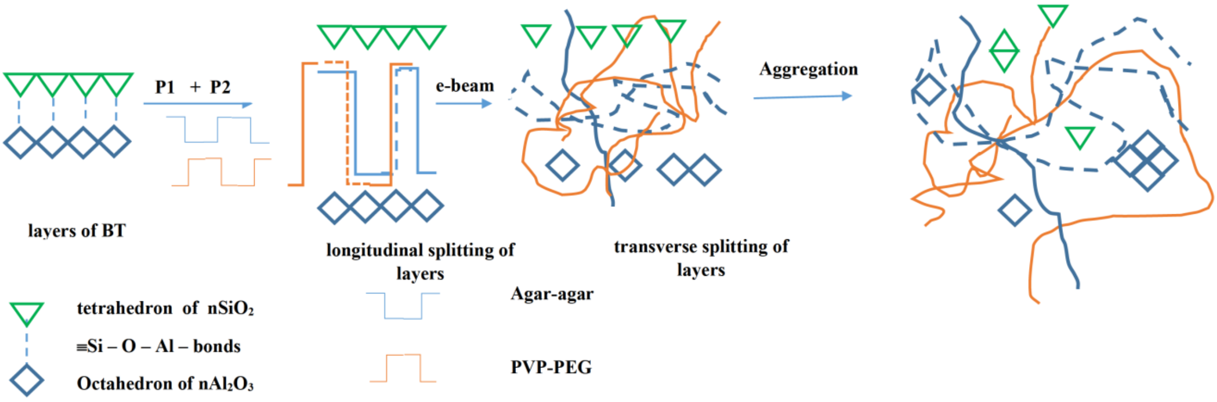

Figure 5. Scheme of exfoliation of bentonite sheets in the IPN matrix
with subsequent ordering of BT crystallites into large aggregates

It can be assumed that during electron irradiation of the P[AA-PVP-PEG]{BT} hybrid composition after partial exfoliation of sheets of mineral filler from each other by the polymer chains begins the stage of aggregation of disordered aluminosilicate sheets with each other along the side faces and edges of aluminum octahedron oxide, forming associates with more or less individual molecules of alumina or silicon oxide or from their linear sequences.

Consequently, recrystallization of bentonite nanoparticles into larger perfect crystals, consisting mainly of aluminum oxide, takes place. The absence of silica tetrahedral structures can be associated with a higher rate of its hydrolysis and dissolution in a water-alcohol medium with formation of polysilicic acid or their associated forms with a polymer matrix through hydrogen bonds according to the scheme compared to aluminum oxide (Fig. 5).

Complete destruction of clay packets in the form of separate sheets leads to formation of a layered structure, which is well distributed in the polymer matrix. This structure provides the most favorable improvement in the characteristics of the resulting polymer nanocomposites in comparison with the intercalated structure due to the high aspect ratio and intense surface reaction of clay particles with polymer chains [31–34].

In addition to the structures of γ-Al_2O_3, SEM micrographs revealed a small number of other geometric configurations (triangular, prismatic, and a number of distorted shapes) belonging to impurity compounds, a detailed study of which is beyond the scope of this article and requires additional in-depth studies.

Previously, the authors [35–37] studied the conditions for production of aluminosilicates by the sol-gel synthesis. It was found that introduction of templates into the aluminosilicate matrix, such as PEG, PEO, cationic surfactants, leads to rapid precipitation of aluminum hydroxide, while two phases of aluminum and silicon oxides condense with no formation of Si–O–Al heterobonds. The resulting octahedra, with an aluminum atom in the center and hydroxyl groups at six corners, has the formula $[Al(OH)_6]^{3-}$.

The molecular composition and structure of the hydrogel compositions produced by the mixing method followed by irradiation with electron beams were identified by IR-Fourier spectroscopy (Fig. 6). Spectra of the three-dimensional polymer matrix P[AA-PVP-PEG] (curve 1) show a clear maximum at 1650 cm^{-1}, corresponding to the stretching vibration band of the carbonyl groups of the pyrrolidone ring, which shifts to the long-wavelength region of 1655 cm^{-1} during three-dimensional radiation polymerization. This indicates the formation of a strong hydrogen bond between the C=O and –OH groups of agar-agar or the terminal hydroxyl groups of PEG, confirming the previously accepted mechanism for the formation of three-dimensional structures in this system [15]. Thus, the synthetic and natural polymers of the hybrid composition are physically intertwined with each other within the three-dimensional framework of PVP and agar-agar, forming an interpenetrating network.

The intensity of the characteristic absorption length of PVP at 2942 cm^{-1}, corresponding to the stretching vibrations of the C–H bond of the methylene groups, increases, indicating a possible superposition of different sections of crosslinked and non-crosslinked sections of polymer chains in the network. Bands of bending vibrations in the region of 1494, 1457, 14221 and 1277 cm^{-1} (C–N-groups) also appear in the spectra of the synthesized polymer hydrogels, which indicates the presence of linear PVP macromolecules, which are associated with both agar-agar and PEG chains.

Figure 6 below shows the Fourier IR spectra of the initial BT (2) and the final hybrid P[AA-PVP-PEG]{BT} (3) composition. It should be noted that the spectra have large overlaps with each other, but it makes it possible to qualitatively identify the structure of the hybrid composition. This is especially evident in the region of 3600–3200 cm^{-1}, which characterizes the stretching vibrations of the hydroxyl groups of both BT and the polymer matrix, including adsorption or capillary water in the composition of the initial matrices. It is also possible to detect the spectra of stretching vibrations of Si–O–Si in the region of 1100– 900 cm^{-1} and deformation vibrations of the Al–O–Al bond in the region of 918 cm^{-1}.

Vibrations in the region of 1018–1046 cm^{-1} can be attributed exclusively to stretching vibrations of the Si–O bond [18, 26]. These results show that chemical interaction occurs between the silicate groups of the inorganic matrix and the functional groups of the polymer matrix, leading to formation of a stable intercalated spatial IPN already from heterogeneous network structures of polymer macromolecules and inorganic ionite P[AA-PVP-PEG]{BT}.

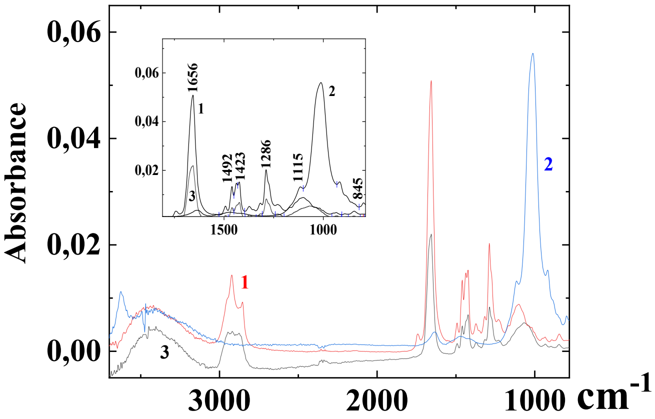

Figure 6. Fourier IR spectra BT (1), P[AA-PVP-PEG] (2) and their hybrid composition P[AA-PVP-PEG]{BT} (3)

Figure 7 shows the swelling kinetics of the compositions P[AA-PVP-PEG]{BT} synthesized in water (1) and in the presence of glycerol with a content of 0.1 wt.% (2) and 0.3 wt.% (3) in the initial reaction mixture. It can be seen that the presence of a low molecular plasticizer of glycerin along with PEG leads to swelling growth of the hybrid composition at the initial time, which can be judged by the tangent of slope angle in this time interval ($tg\alpha = \Delta K_{sw}/\Delta t$). So for the composition synthesized in water ($tg\alpha$=15.87°), in 0.1 and 0.3 wt.% glycerol is 9.963 and 7.53, respectively. Swelling profile in water and 0.1 wt. % glycerol has bends in the range from 0.5 to 1.5 hours, which may be defined by gradual hydration of the composition components when water molecules penetrate into its volume through the pores of the polymer matrix. It should be assumed that, first of all, fragments of the polymer matrix will be subjected to hydration, in particular, macromolecules of natural polysaccharide and PVP associated with PEG-400 chains through a system of hydrogen bonds, as noted above. The presence of a bend corresponds to the site when hydration of the mineral filler bentonite begins, the particles of which are distributed in the areas between the crosslinking nodes of the polymer matrix components. With a glycerol content of 0.3 mass. %, such bend is not observed, which may be caused by a change in the structure of bentonite with an excess content of glycerol in the composition of the initial mixture.

We believe that at a low content of glycerol ($\omega_{ГЦ} < 0.1$ wt.%), there is a maximum flaking of aluminosilicate sheets from each other with the growth of interplanar distance between them in bentonite particles. This gives maximum rigidity to the polymer matrix they are located in. With the growth of glycerol content to 0.3 wt.%, its function from the expansion factor of the interplanar distance between the sheets changes to the function of a plasticizer, when its excess amount begins to bind to the hydrophilic ridges of the matrix macromolecules and the oxygen atoms of the aluminosilicate groups of bentonite due to hydrogen bonds. In this case, the interplanar spacing between the aluminosilicate layers can approach in value the initial parameters of the matrix with no glycerol additives due to enhancement of hydrophobic interactions stabilized by a system of hydrogen bonds. This can explain the twofold increase in the swelling coefficient of hybrid composition material in the presence of 0.1 wt. % glycerol.

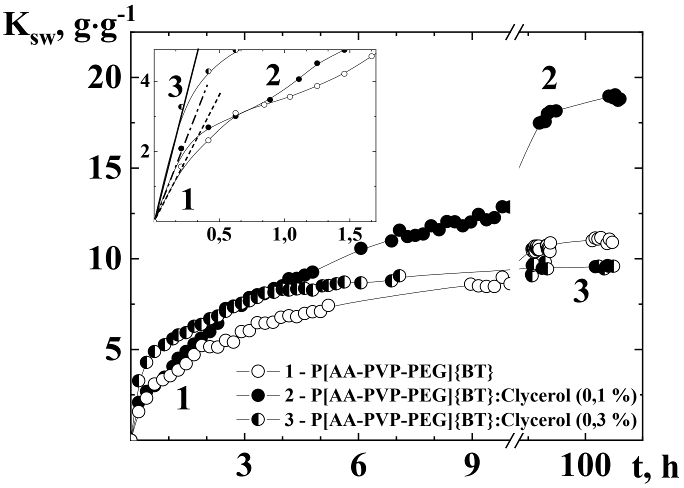

Figure 7. Change in the swelling coefficient of hydrogels P[AA-PVP-PEG]{BT} at different glycerol content

This conclusion is in good agreement with the results of strength measurements for hybrid composite materials. The strength properties and deformation behavior of hydrogel compositions are clearly illustrated by the stress–strain dependence (P = *f* (ε)), obtained by the method for determining the "puncture" strength of a material by pressing a ball through a layer of a flat composite hydrogel. Three main sections can be distinguished on the deformation curves (Fig. 8). The initial, gently sloping rectilinear section corresponds to the area of plastic, the second — to elastic, the third — to viscous-flowing deformation. In the interval of sections II–III, phase transitions and orientation of macromolecular chains take place between crosslinking sites in the direction of the applied tension and compression force, at which the segment mobility of macromolecules increases and the structure of the material is rearranged. In section III, the relaxation rate of the material becomes comparable with the strain rate of the sample. Outside the zone III, with further deformation, macrocracks appear in the sample of hydrogel composition, as a result, the thinning section of the composite hydrogel, which bears the load from the indented ball, is punctured from region I to region III [15].

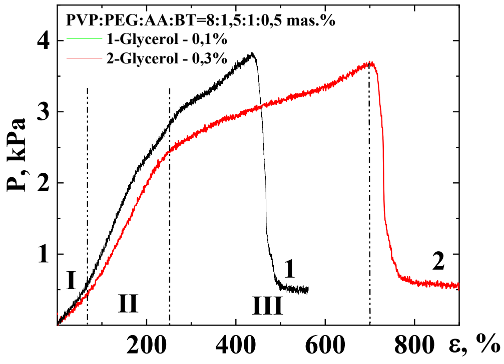

Figure 8. Deformation curves of hybrid composite materials P[AA-PVP-PEG]{BT} at different glycerol content

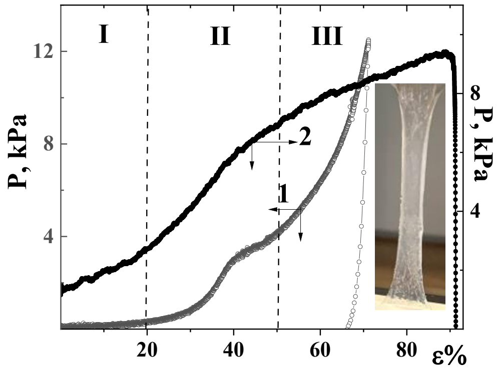

Figure 9. Stress-strain dependence of the composition **P**[AA-PVP-PEG]{BT}

It can be seen that when the content of glycerol in the hybrid composition is 0.1 wt. %, it shows a noticeable increase in the strength of material from 3680 Pa to 3834 Pa with a decrease in the strain value from 693% to 400% compared to the sample, where its content is 0.3 wt. %. This indicates an increase in interplanar distances between aluminosilicate sheets and the space between them is filled predominantly by the vertically oriented glycerol molecules. This leads to an increase in the disjoining pressure and stress, which affects the ultimate strength of the material and reduces its deformation during punching.

With the growth of glycerol content between sheets of aluminosilicates in bentonite particles, hydrophobic interactions increase and the material acquires viscous-flowing properties against the background of a slight decrease in puncture strength.

Figure 9 shows the stress-strain dependence for uniaxial compression (curve 1) and tension (curve 2) of a cylindrical and rectangular sample, respectively. Under uniaxial compression, the dependence $P = f(\varepsilon)$ shows a break in the deformation range of ~30 % followed by a smooth increase in stress up to 12 kPa at $\varepsilon = 70$ %.

It is important to have a qualitative representation of the process leading to strengthening or weakening of the strength of the composite material under external loads to establish quantitative relationships between the structure and the property of a material to resist destruction. It is now generally known that absorption of the energy transferred to the polymer matrix occurs almost entirely. The function of fillers-plasticizers is to promote and control deformations in the matrix, providing significant stress concentrations in those places where local deformations can be initiated. Shear fluidity plays a role in the process, but crazing is the predominant hardening mechanism. Many researchers have shown that stress whitening is associated with formation of more crazes than microcracks [35].

With regard to the system we are considering, it can be assumed that mineral fillers play the role of stress absorbers caused by compression or tension of the sample.

The stress-strain dependence does not show a region of elastic deformation corresponding to the Hooke model. The dependence $P–f(\varepsilon)$ already at the initial stages resembles a plastic deformation profile, that is, not a sharp, but a gentle change in shear or compression stress up to $\varepsilon \approx 20$ %, which is not typical for most previously studied systems [38]. When a sample is compressed in the region of $\varepsilon \in 30–50$ % there is a “consistent” orientation of mineral particles and layers of polymeric planes of a three-dimensional matrix, along the axis of tension or compression. It is natural in this case to expect some change in the morphological structure of the hybrid composition, which corresponds to the bend section on the stress-strain curve during compression, which is not observed in the absence of a mineral filler [15]. Such bends correspond to the region of the conformational transition of macromolecules “coil-globule” [38, 39].

Any parameter that affects the degree of intercalation and delamination, like the modulus, has a significant effect on the tensile strength of nanocomposites. Another effect of the nanoclay filler on the mechanical characteristics of nanocomposites is the value of elongation at break, which is affected by the interfacial reaction between the polymer and layered silicates [40].

In addition, introduction of a mineral filler into the volume of the polymer matrix resulted in a decrease in the degree of elongation by almost a factor of two [15]. In shear zones [38], molecules are oriented approximately parallel to the applied tensile stress and, therefore, normal to the planes where crazes form. Since both the initiation and growth of crazes are inhibited due to orientation in this direction, shear bands have an effect on inhibition of the crazes growth. As the number of shear bands increases, the length of newly formed crazes decreases, which is shown in the image (Figure 9).

Provision of the exfoliation conditions is of particular importance as it maximizes the interaction between the polymer and the clay particles, allowing the polymer to access the entire surface of the silicate layers, thus leading to the greatest changes in various physical properties. Nevertheless, there are still disputes about whether the system of polymer–clay nanocomposites contains entirely layered silicates, which is confirmed by the fact that a significant part of polymer nanocomposites in the literature has intercalated or mixed intercalated–layered nanostructures [41]. This is due to the fact that silicate layers are highly anisotropic, their side sizes vary from 100 to 1000 nm, and they cannot be arranged randomly in the polymer matrix even when separated at a large distance from each other [42].

In the course of crazing processes during sample stretching in tension, according to formation of microcracks in the area of material fastening and whitening in the central part from the fastening periphery, the shear stress is concentrated at break. Moreover, in the studied polymer compositions the formation of a “neck” is not observed, and the system rather passes into a viscous-fluid state than into a highly elastic state before destruction of the sample.

Most studies show that elastic modulus of polymer nanocomposites, fabricated using modified organoclay growth significantly, especially at increasing of load on the organoclay [43]. However, in some cases, the Young's modulus decreased, since completely exfoliated structures are replaced by partially exfoliated intercalated structures when the volume fraction of organoclay exceeds the threshold limit value [44, 45].

We propose to consider such hybrid composite materials as a new class of interpenetrating networks with promising applied properties (materials for tissue engineering and anti-burn hydrogel dressings with a wound healing effect and high bactericidal activity, etc.).

Conclusions

Thus a systematic study of the synthesis of hybrid composite materials based on synthetic (PVP) and natural (AA) macromolecules in the presence of plasticizers (PEG-400, glycerol) and the mineral filler bentonite was carried out.

X-ray diffraction analysis and SEM showed that the structure of the resulting hybrid compositions is defined as an interpenetrating network, in the volume of which intercalated particles of the mineral component are distributed.

It has been established that the mechanical properties of the hybrid composition are determined mainly by structural organization of the interpenetrating polymer network formed during electron irradiation of the initial polymer mixture in the presence of plasticizers, as well as by the conditions for intercalation of polymer segments into the interpacket layers of the mineral matrix. During the process of crazing of the sample under tension the shear stress is concentrated in the central part of the sample from the periphery of the fastening.

It is shown that the degree of swelling of the hybrid composition strongly depends on concentration of a low molecular plasticizer in the polymeric interpenetrating network, which can easily impregnate into the interplanar layers of bentonite.

Acknowledgements

The work was carried out within the framework of the Program “Development of nuclear physics methods and technologies for innovative modernization of the economy of Kazakhstan” (2021– 2023) of the Ministry of Energy of the Republic of Kazakhstan (state registration number 0121RK00656, IRN number BR09158958).

The authors express their gratitude to LPP “Institute of Polymer Materials and Technologies” for providing the opportunity to measure mechanical characteristics of hybrid compositional materials.

References

1 Albdiry, M.T., Yousif, B.F., Ku, H., Lau, K.T (2013). A critical review on the manufacturing processes in relation to the properties of nanoclay/polymer composites. *J. Compos. Mater., 47*, 1093–1115. https://doi.org/10.1177/0021998312445592

2 Du, J.H., Cheng, H.M (2012). The fabrication, properties, and uses of graphene/polymer composites. *Macromol. Chem. Phys. 213*, 1060–1077. https://doi.org/10.1177/0021998312445592.

3 Müller, K., Bugnicourt, E., Latorre, M., Jorda, M., EchegoyenSanz, Y., Lagaron, J.M., Miesbauer, O., Bianchin, A., Hankin, S., Bölz (2017). Review on the processing and properties of polymer nanocomposites and nanocoatings and their applications in the packaging, automotive and solar energy fields. *Nanomaterials, 7*, 74. https://doi.org/10.3390/nano7040074

4 Valapa, R.B., Loganathan, S., Pugazhenthi, G., Thomas, S., Varghese, T.O. (2017) An Overview of Polymer-Clay Nanocomposites. In *Clay-Polymer Nanocomposites*, Amsterdam, The Netherlands: Elsevier.; pp. 29–81, ISBN: 978-0-323-46153-5. https://doi.org/10.1016/B978-0-323-46153-5.00002-1

5 Kotal, Moumita., Bhowmick A. (2015). Polymer nanocomposites from modified clays: Recent advances and challenges. *Progress in Polymer Science, 51*, 127–187. https://doi.org/10.1016/j.progpolymsci.2015.10.001

6 Lee, K.-Y., Aitomäki, Y., Berglund, L.A., Oksman, K., Bismarck, A. (2014). On the use of nanocellulose as reinforcement in polymer matrix composites. *Compos. Sci. Technol., 105*, 15–27. https://doi.org/10.1016/j.compscitech.2014.08.032

7 Zhang, J., Manias, E., Wilkie, C.A. (2008). Polymericallymodified layered silicates: An effective route to nanocomposites. *J. Nanosci.Nanotechnol., 8*, 1597–1615.

8 Nosonovsky, M., Bhushan, B. (2010). Green tribology: Principles, research areas and challenges. *Philos. Trans. R. Soc. A math. Phys. Eng. Sci., 368*, 4677–4694. https://doi.org/10.1098/rsta.2010.0200

9 Kasprzhitsky, A.S., Morozov, A.V. Lazorenko, G.I., Talpa, B.V., Yavna, V.A. (2013). Complex study of the composition and structural features of rock-forming minerals of bentonite clays of the Millerovsky deposit. *Engineering Bulletin of Don., 3*, 26. https://cyberleninka.ru/article [in Russian].

10 Mamidi, N., Gamero, M.R.M., Villela-Castrejón, J., Elías-Zúníga, A. (2019). Development of ultra-high molecular weight polyethylene functionalized carbon nano-onions composites for biomedical applications. *Diam. Relat. Mater. 97*, 107435. https://doi.org/10.1016/j.diamond.2019.05.020

11 Gylymkhan, N.T., Zhumagalinva, Sh.N., Abilov, Zh.A. (2016). Possibilities of using bentonite clays in medicine. Report NAS RK, 4, 24–33 [in Russian].

12 Tiwari, J.N., Tiwari, R.N., Kim, K.S. Zero-dimensional, one-dimensional, two-dimensional and three-dimensional nanostructured materials for advanced electrochemical energy devices. (2012). *Prog. Mater. Sci., 57*, 724–803. https://doi.org/10.1016/j.pmatsci.2011.08.003

13 Chan, J.X., Wong, J.F., Petru, M., Hassan, A., Nirmal, U., Othman, N., Ilyas, R.A. (2021). Effect of Nanofillers on Tribological Properties of Polymer Nanocomposites: A Review on Recent Development. *Polymers., 13,* 2867. https://doi.org/10.3390/polym13172867

14 Pavlidou, S., Papaspyrides, C.D. (2008). A review on polymer–layered silicate nanocomposites. *Prog. Polym. Sci., 33,* 1119–1198. https://doi.org/10.1016/j.progpolymsci.2008.07.008

15 Alexandre, M., Dubois, P. (2008). Polymer-layerd silicate nanjcjmposites: preparation, properties and uses of a new class of materials. *Material Science and Engineering, 28*, 1–63. https://doi.org/10.1016/S0927-796X(00)00012-7

16 Mamytbekov, G., Beksultanov, Z., Bannykh, V. (2022). Synthesis, structure and mechanical properties of composite hydrogels for medical applications. *Chemical Bulletin of the Kazakh National University, 104* (1), 30–42. https://doi.org/https://doi.org/10.15328/cb1264

17 Dalia, E. Abulyazied, Antoaneta E. (2021). Investigative Study on the Progress of Nanoclay-Reinforced Polymers: *Preparation, Properties, and Applications. Review Polymers, 13,* 4401. https://doi.org/10.3390/polym13244401

18 Zhu, W., Chu-Hua, L., Chang, F.-C., Kuo, S.-W. (2012) Supramolecular ionic strength-modulating microstructures and properties of nacre-like biomimetic nanocomposites containing high loading clay. *RSC Adv., 2,* 6295–6305. https://doi.org/10.1039/c2ra20523h

19 Gordeeva, N.V., Tolmachev, I.A., Mashlyakovsky, L.N., Vasiliev, V.K. (2012). Influence of nanoparticles of layered silicates on the properties of aqueous dispersions of acrylate copolymers and films based on them. *Proceedings of the St. Petersburg State Technological Institute (Technical University), 14,* 41–44.

20 Botana, A., Mollo, M., Eisenberg, P., & Sanchez, R. M. T. (2010). Effect of modified montmorillonite on biodegradable PHB nanocomposites. *Applied Clay Science, 47* (3–4), 263–270. https://doi.org/10.1016/j.clay.2009.11.001

21 Srinivasan, R. (2011). Advances in Application of Natural Clay and Its Composites in Removal of Biological, Organic, and Inorganic Contaminants from Drinking Water. *Advances in Materials Science and Engineering. Article ID 872531*, 17. https://doi.org/10.1155/2011/872531

22 Maršálek, R., Navrátilová, Z. (2011). Comparative study of CTAB adsorption on bituminous coal and clay mineral. *Chemical Papers., 65* (1), 77–84. https://doi.org/10.2478/s11696-010-0076-9

23 Fischer, H. Polymer nanocomposites: from fundamental research to specific applications (2003). *Materials Science and Engineering: C, 23* (6-8), 763–772. https://doi.org/10.1016/j.msec.2003.09.148

24 Nagornov, R. S., Razgovorov, P. B., Smirnova, E. A., Razgovorova, M. P. (2015). Complex extraction of biologically active ingredients from oil-containing media using mineral sorbents. *Chemistry and Medicine*: Abstract of report of X All-Russian conference with international participation. In-t org. Chemistry USC RAS. Ufa-Abzakovo: Gilem.

25 Galan, E., Singer A. (2011). *Developments in Palygorskite-Sepiolite Research. A New Outlook of these Nanomaterials*, Oxford-Amsterdam: Elsevier. ISSN 1572-4352. https://doi.org/10.1016/1B978-0-444-53607-5.00001-3

26 Tarasevich, Yu. I., (1988). *Structure and chemistry of the surface of layered silicates*. Kyiv, Nauk. dumka [in Russian].

27 Greg, S., Sing, K. (1984). *Adsorption, specific surface area, porosity*: Translation from English. Moscow: Mir [in Russian].

28 Bonilla-Petriciolet, A., Mendoza-Castillo, D.-I., ReynelÁvila, H.-E. (2017). *Adsorption Processes for Water Treatment and Purification*. Cham.: Springer, 2017. https://doi.org/10.1007/978-3-319-58136-1

29 Gerasin, V.A., Antipov, E.M., Karbushev, V.V., Kulichikhin, V.G., Karpacheva, G.P., Talroze, R.V., Kudryavtsev, Ya.V. (2013). New approaches to creation of hybrid polymer nanocomposites: structural materials to high-tech applications. *Advances in Chemistry, 82* (4), 303–332. https://doi.org/10.1070/RC2013v082n04ABEH004322

30 Kupchishin A.I., Taipova B.G. (2018). Various models of destruction of polymeric materials and composites by electron beams. *NNC RK Bulletin, 4*, 107–110 [in Russian].

31 Kausar, A. (2020). A review of fundamental principles and applications of polymer nanocomposites filled with both nanoclay and nano-sized carbon allotropes-graphene and carbon nanotubes. *J. Plast. Film Sheeting, 36*, 209–228. https://doi.org/10.3390/polym13244401

32 Jose, A.J., Alagar, M. 3 - Preparation and characterization of polysulfone-based nanocomposites (2015). *Manufacturing of Nanocomposites with Engineering Plastics*, 31-59. https://doi.org/10.1016/B978-1-78242-308-9.00003-3

33 Ke, Y.C., Stroeve, P. (2005). Polymer-Layered Silicate and Silica Nanocomposites; Elsevier: Amsterdam, The Netherlands, ISBN 0080457584.

34 Kumar, A., Zhang, R., Venkatesan, M., Stamenov, P., Coey, J.M.D. (2022). Exfoliation of hematite: Morphological, structural and magnetic investigations. *J. Magn. Magn. Mater., 542*, 168507. https://doi.org/10.1016/j.jmmm.2021.168507

35 Hernandez, C., Pierre, A.C. (2001). Evolution of the texture and structure of SiO_2-Al_2O_3 xerogels and aerogels as a function of the Si to Al molar ratio. *J. of sol-gel science and technology, 20*, 227–243. https://doi.org/10.1023/A:1008714617174

36 Gordeeva, N.V., Tolmachev, I.A., Mashlyakovsky, L.N., Vasiliev, V.K. (2012). Influence of nanoparticles of layered silicates on the properties of aqueous dispersions of acrylate copolymers and films based on them. *Proceedings of the St. Petersburg State Technological Institute (Technical University), 14*, 41–44.

37 Sun, Q., Joseph Schork F., Deng, Y. (2007). Water-based polymer/clay nanocomposite suspension for improving water and moisture barrier in coating. Composites *Science and Technology, 67(9)*, 1823–1829. https://doi.org/10.1016/j.compscitech.2006.10.022

38 Paul, D., Newman, S. (Eds.) (1978). *Polymer blends,* NY, USA: Academic Press. https://doi.org/10.1016/B978-0-12-546802-2.X5001-5

39 Morawetz, H. (1975). *Macromolecules in solution.* New York: Wiley. https://doi.org/10.1002/pol.1976.130140914

40 Burmistr, M.V., Skhyy, K.M., Shilov, V.V., Pissis, P., Spanoudaki, A., Sukha, I.V., Tomilo, V.I., Gomza, Y.P. (2005). Synthesis, structure, thermal and mechanical properties of nanocomposites based on linear polymers and layered silicates modified by polymeric quaternary ammonium salts (ionenes). *Polymer, 46,* 12226–12232. https://doi.org/10.1016/j.polymer.2005.10.094

41 Jamshidian, M., Tehrany, E.A., Imran, M., Akhtar, M.J., Cleymand, F., Desobry, S. (2012). Structural, mechanical and barrier properties of active PLA-antioxidant films. *J. FoodEng., 110,* 380–389. https://doi.org/10.1016/j.jfoodeng.2011.12.034

42 Ali, F., Ullah, H., Ali, Z., Rahim, F., Khan, F., Rehman, Z.U. (2016). Polymer-clay Nanocomposites, Preparations and Current Applications: A Review. *Curr. Nanomater., 1,* 83–95. https://doi.org/10.2174/2405461501666160625080118

43 Motawie, A.M., Madani, M., Esmail, E.A., Dacrorry, A.Z., Othman, H.M., Badr, M.M., Abulyazied, D.E. (2014). Electrophysical characteristics of polyurethane/organo-bentonite nanocomposites. *Egypt. J. Pet., 23,* 379–387. https://doi.org/10.1016/j.ejpe.2014.09.005

44 Chen, B. (2004). Polymer-clay nanocomposites: An overview with emphasis on interaction mechanisms. Br. Ceram. Trans. *103,* 241–249. https://doi.org/10.1179/096797804X4592

45 Shokrieh, M.M., Kefayati, A.R., Chitsazzadeh, M. (2012). Fabrication and mechanical properties of clay/epoxy nanocomposite and its polymer concrete. Mater. Des. 40, 443-452. http://dx.doi.org/10.1016/j.matdes.2012.03.008

Ғ.Қ. Мамытбеков, Ж.И. Бексултанов, В.И. Банных, И.В. Данько

Бентонит негізіндегі гибридті композициялық материалдардың синтезі, құрылымы және қасиеттері

Пластификаторлар (ПЭГ-400, глицерин) мен бентнонит минералды толтырғыштарының қатысуымен синтетикалық (поли-N-винилпирролидон) және табиғи (агар-агар) макромолекулалардың негізінде гибридті композициялық материалдарды электрондық сәулелену әдісімен синтездеу процесі жүйелі зерттелді. РСА және СЭМ әдістері көмегімен алынған гибридті композициялардың құрылымы минералды компоненттердің интеркалирленген бөлшектерінің өзара өтімді тор ретінде қарастыруға болатындығы анықталды. Бентонит-өзара өтімді тор гибридті құрамы қалыптасу кезінде минералды толтырғыштың бөлшектері өзара өтімді тордың қабаттарнның арасы бойынша біркелкі бөлінбейді. Гибридтік композицияның механикалық қасиеттері пластификаторлардың қатысуымен бастапқы полимер қоспасының электронды сәулеленуі кезінде пайда болатын өзара өімді полимер торының негізгі құрылымдылығымен, сондай-ақ полимер сегменттерінің минералды төсеніштің тораралық қабаттарына интеркаляция жағдайымен анықталады. Үлгіні созу кезінде крейзинг процесінде созылу кезінде ығысу кернеуі үлгінің бекіту перифериясынан орталық бөлігіне шоғырланады. Гибридті композицияның ісіну дәрежесі бентониттің аралық қабаттарына оңай ене алатын полимерлі өзара өтімді тордың құрамындағы төмен молекулалы пластификатордың концентрациясына байланысты екендігі көрсетілген.

Кілт сөздер: гибридті композициялық материалдар (ГКМ), полимерлік-бейорганикалық композициялар (ПБК), электрондық сәулелену, синтетикалық және табиғи полимерлер, бентонит, деформация, қысу, созылу, интеркаляция, өзара өтімді торлар (IPN).

Г.К. Мамытбеков, Ж.И. Бексултанов, В.И. Банных, И.В. Данько

Синтез, структура и свойства гибридных композиционных материалов на основе бентонита

Проведено систематическое исследование процесса синтеза гибридных композиционных материалов на основе синтетического (поливинил-N-пирролидон) и природного (агар-агар) макромолекул в присутствии пластификаторов (ПЭГ-400, глицерин) и минерального наполнителя бентонита методом электронного облучения. Методами РСА и СЭМ показано, что структура полученных гибридных композиций определяется как взаимопроникающая сетка (ВПС), в объеме которой распределены интеркалированные частицы минеральной компоненты. При формировании гибридной композиции бентонит-ВПС частицы минерального наполнителя неравномерно распределяются по межслоевым поверхностям взаимопроникающей сетки. Установлено, что механические свойства гибридной композиции определяются преимущественно структурной организацией взаимпроникающей полимерной сетки, формирующейся в ходе электронного облучения исходной полимерной смеси в присутствии пластификаторов, а также условиями интеркалляции полимерных сегментов в межпакетные слои минеральной матрицы. В ходе процессов крейзования при растяжении образца происходит концентрирование напряжения сдвига в центральную часть образца от периферии крепления при разрыве. Показано, что степень набухания гибридной композиции сильно зависит от концентрации низкомолекулярного пластификатора в составе полимерной взаимопроникающей сетки, которая может легко импрегнировать в межплоскостные слои бентонита.

Ключевые слова: гибридные композиционные материалы (ГКМ), полимерно-неорганические композиции (ПНК), электронное облучение, синтетические и природные полимеры, бентонит, деформация, сжатие, растяжение, интеркаляция, взаимопроникающие сети (ВПС).

Information about the authors*

Mamytbekov, Galymzhan Kulamkadyrovich (*corresponding author*) — Doctor of Chemical Sciences, Full Professor, Chief researcher, Center for Complex Environmental Research, Institute of Nuclear Physics, Ibragimov St., 1, 050032, Almaty, Kazakhstan, e-mail: g.mamytbekov@inp.kz; https://orcid.org/0000-0003-3848-3709;

Beksultanov, Zhomart Imuchanbetovich — Head of Research and Production Center for Radiation Technologies, Institute of Nuclear Physics, Ibragimov St., 1, 050032, Almaty, Kazakhstan, e-mail: bek@inp.kz; https://orcid.org/0000-0002-4778-5023;

Bannykh, Valentina Ivanovna — Head of the Quality Control Group, Institute of Nuclear Physics, Ibragimov St., 1, 050032, Almaty, Kazakhstan, e-mail: v.bannykh@inp.kz; https://orcid.org/0000-0002-2779-6390;

Dan’ko, Igor Vitalievich — Deputy Head of the Scientific and Technical Department of Accelerator Technologies, Institute of Nuclear Physics, Ibragimov St., 1, 050032, Almaty, Kazakhstan, e-mail: i.danko@inp.kz; https://orcid.org/0000-0001-7377-5913

---

*The author's name is presented in the order: *Last Name, First and Middle Names*